THE FOURIER METHOD

R. KOSLOFF
Department of Physical Chemistry and
The Fritz Haber Research Center for Molecular Dynamics
The Hebrew University
Jerusalem 91904
Israel

ABSTRACT. A survey of the basic features of the Fourier method for a grid represention of quantum mechanical wavefunctions is presented. The intention is to gain insight into the connection between the mathematical foundations and the physical applications. The elements of functional representation theory are explored to uncover the roots of the Fourier representation method for molecular dynamics. The method is viewed in the context of orthogonal collocation methods. The representation of nonlocal operators is reviewed. The Harmonic oscillator is used as an illustration for a discussion of sampling optimization. Some more advanced topics such as mapped representations and multidimensional generalizations are also discussed.

1. Representation theory

Representation theory can be thought of as a setting of the stage on which dynamical events can take place. In quantum mechanics this stage supplies the mathematical framework necessary to represent the state of a system and its evolution through time. In other words, by following the evolution of the state of the system the values of measurements can be extracted. Axiomatic quantum mechanics which originated in the work of von Neumann bases the description of the state in Hilbert space [1]. Three elements constitute this Hilbert space: a) A functional domain with well-defined boundary conditions. b) A set of vectors defined on this functional domain; the definition of the scalar product of two vectors is a crucial element. c) Operators which map the vectors into new ones in the same functional domain.

A molecular encounter can be imagined as taking place in a large multi-dimensional "box" which is a product of the momentum coordinate phase space box and the time energy phase space. This view is consistent with the practical observation that any experiment is contained in a finite volume, is restricted to an energy band which also determines the momentum range, and is completed in finite time. Such a view is reflected in the methods of simulation which impose a finite representation of space-momentum, time-energy phase space. It becomes apparent therefore that the computational effort is determined by the "volume" of this box in phase space and a central point when considering computational methods is their ability to represent the volume effectively. The global nature of quantum mechanics requires that the box should be globally represented. This fact is responsible for the large memory requirements of quantum computational schemes. In the construction of a calculation scheme a restriction to a discrete representation has to be imposed on the Hilbert space.

Consider approximating an arbitrary function $\psi(x)$ by a finite set of N functions $g_n(x)$

$$\psi(x) \approx \tilde{\psi}(x) = \sum_{n=0}^{N-1} a_n \, g_n(x) \, , \tag{1}$$

where $g_n(x)$ are analytic functions in the domain of interest. The finite representation problem is recast as a method to optimize the expansion coefficients a_n. The traditional approach is the variation method which minimizes the functional

C.Cerjan (ed.), Numerical Grid Methods and Their Application to Schrödinger's Equation, 175–194.

$$J = \int_D d\mathbf{x}\ |\psi(x) - \bar{\psi}(x)|^2 \ . \tag{2}$$

Here, J is the averaged squared difference between the function ψ and its approximation $\bar{\psi}$, and D is the domain of interest, leading to the determination of a_n by the relation $\delta J = 0$. If the expansion functions are orthogonal, $< g_n | g_m >= \delta_{nm}$, then the expansion coefficients become the functional transform of ψ: $a_n = < \psi | g_n >$. This method will be referred to as the variational spectral method [2]. An alternative approach, due to Gauss, is the collocation technique for optimizing the expansion coefficients. This technique will be explored in the next section.

2. General Collocation Method

Imagine viewing the functional space through a finite set of portholes which restrict the view to a local picture. If these portholes are dense enough, a complete picture can be reconstructed by using the continuous properties of the functional space to interpolate the observed data and reconstruct the full picture. The collocation method makes use of this concept. In mathematical terms the collocation method determines the expansion coefficients by matching the approximate solution to the true solution on a set of N grid points,

$$\psi(x_j) \equiv \bar{\psi}(x_j) = \sum_{n=0}^{N-1} a_n\ g_n(x_j) \ , \tag{3}$$

where the x_j are the collocation points. These are the sampling points discussed above. This equation is equivalent to a set of coupled linear equations. In matrix form they become

$$\psi = \mathbf{G}\ \mathbf{a} \ , \tag{4}$$

where $\psi_j = \psi(x_j)$ and the matrix $G_{nj} = g_n(x_j)$. Provided that the $g_n(x_j)$ are linearly independent, the solution becomes

$$\mathbf{a} = \mathbf{G}^{-1}\ \psi \ . \tag{5}$$

The functional basis that supplies the global picture is connected through the expansion coefficients a_n to the spatial grid. This provides the ability to define the scalar product of two functions. If

$$\psi(x) = \sum_n a_n g_n(x) \tag{6}$$

and

$$\phi(x) = \sum_m b_m g_m(x) \tag{7}$$

then

$$< \psi | \phi > \equiv \sum_{nm} S_{nm} a_n^* b_m \tag{8}$$

where S_{nm} is the overlap matrix

$$S_{nm} = \int_D dx\ g_n(x)^* g_m(x) \tag{9}$$

and the integration is carried out over the domain D.

The operators in the discrete Hilbert space can be represented by its expression in terms of the expansion coefficients. The duality of unbounded operators, quantified by the uncertainty principle, implies that the local, point-wise, evaulation of the potential forces the momentum operator to become nonlocal. Hence, the accurate evaulation of nonlocal operators, such as the momentum operator $-i\hbar\frac{\partial}{\partial x}$ and its mapping of the wavefunction $\psi(x)$ becomes crucial

$$-i\hbar\frac{\partial}{\partial x}\psi(x) \approx -i\hbar\sum_{n=0}^{N-1} a_n \frac{\partial}{\partial x}g_n(x) . \tag{10}$$

The action of these nonlocal operators can be reduced to a calculation at the sampling points x_j,

$$-i\hbar\frac{\partial}{\partial x}\psi(x_j) \approx -i\hbar\sum_{n=0}^{N-1} a_n\, q_n(x_j) , \tag{11}$$

by defining new expansion functions $q_n(x) = \frac{\partial}{\partial x}g_n(x)$. Usually these new functions $q_n(x)$ are recast into a linear combination of the old ones $g_n(x)$, resulting in a discrete representation of the non local operation. The duality of the representation which, on the one hand is represented by the values at sampling points and on the other by a functional global representation, is responsible for the applicability of the method to represent processes in Hilbert space. Thus either the sampling points or the functional expansion can be taken as the "fundamental" representation with a linear mapping connecting them – the matrix **G** above.

Primitive collocation methods which use nonorthogonal expansion functions have been used. An example is the method of Hamilton and Light [3] which uses a set of distributed Gaussians as expansion functions, $g_n(x)$. The main numerical drawback of primitive collocation schemes is overcompleteness of the representation leading to a reduction in the rank of the overlap matrix S. This problem causes numerical singularities in the inversion of the **G** matrix. This phenomenon can also be understood from the perspective of Gram-Schmidt orthogonalization. Functions which have nearly complete overlap will cause extreme numerical sensitivity upon orthogonalization. One way to overcome this problem is to use orthogonal expansion functions, the subject of the next section. Another method is to use more sampling points than functions and a least square procedure to overcome the indeterminancy of the inversion.

3. Orthogonal Collocation Schemes

A great simplification in the collocation scheme is achieved if the set of expansion functions $g_n(x)$ obeys the orthogonality relation

$$\sum_{n=0}^{N-1} g_n(x_i)g_n^*(x_j) = \delta_{ij} , \tag{12}$$

allowing a direct inversion for the coefficients a_n in equation (4)

$$a_n = \sum_j \psi(x_j)g_n^*(x_j) . \tag{13}$$

This means that the expansion coefficients a_n are the discrete functional transform of the function ψ. On the other hand if

$$< g_n|g_m > = \int_D dx\; g_n(x)g_m^*(x) = \delta_{nm} \tag{14}$$

then the scalar product in equation (8) is greatly simplified leading to

$$< \psi|\phi > \; = \; \sum_n a_n{}^* b_n \tag{15}$$

which, using equation (12), becomes

$$< \psi|\phi > \; = \; \sum_{j=0}^{N-1} \psi^*(x_j)\phi(x_j) \; . \tag{16}$$

A consequence of the orthogonality relations is that the collocation functional expansion scheme becomes a discrete vector space with a unitary transformation between the discrete sampling points x_j and the discrete functional base a_n. The matrix $\mathbf{G}$ is unitary. The following sections will elaborate on a particular choice of orthogonal functions: the Fourier set. Other orthogonal functions, especially orthogonal polynomials, have been used successfully in some applications. These choices are explored in other chapters [4].

4. The Fourier Method In 1D

An examination of the Fourier method, which is a special case of an orthogonal collocation representation, elucidates the main considerations of representation theory. It will be shown that by optimizing the representation the quantum limit of one point per unit phase space volume of h can be obtained. Moreover, the Fourier method has great numerical advantages because of the "fast" nature of the algorithm [5]. This means that the numerical effort scales semilinearly with the represented volume of phase space.

In the Fourier method, the orthogonal functions $g_n(x)$ are chosen as

$$g_k(x) \; = \; e^{i2\pi kx/L} \; , \quad k \; = \; -(N/2-1), ..., 0, ..., N/2 \tag{17}$$

leading to N equally spaced sampling points where $x_j \; = \; (j-1)\Delta x$, $(j \; = \; 1, ...N)$ and L is the length of the interval. Using the relation $L \; = \; N\Delta x$, the completeness relations of the Fourier expansion functions become

$$\sum_{k=-N/2-1}^{N/2} g_k(x_n)g_k^*(x_m) \; = \; \sum_{k=-N/2-1}^{N/2} e^{i2\pi kx_n/L}e^{-i2\pi kx_m/L} \; =$$

$$\sum_{k=-N/2-1}^{N/2} e^{i2\pi kn/N}e^{-i2\pi km/N} \; = \; \frac{1-e^{i2\pi(n-m)}}{1-e^{i2\pi(n-m)/N}} \tag{18}$$

where the summation can be carried out explicitly because it is a geometric series. The fourth equality in equation (18) follows because if $n \; = \; m$ the summation is trivial. Otherwise, $|n-m|$ ranges from 1 to $N-1$ and is never an integral multiple of N. Thus the denominator never vanishes while the numerator is identically zero. This is the first orthogonality relation equation (12).

The second orthogonality relation equation (14) becomes

$$\frac{1}{2\pi}\int_{-\pi}^{\pi} e^{imx'}e^{-inx'}dx' \; = \; \frac{1}{2\pi}\left[\; \frac{1}{i(m-n)} \; e^{i(m-n)x} \; \right]_{-\pi}^{\pi} \; = \; \delta_{nm} \tag{19}$$

where $x' = \pi(x/L - 1)$, $0 \leq x \leq L$. These relationships imply that the domain D has periodic boundary conditions. The symmetry between n and k in equation (18) leads to the discrete version of equation (19):

$$\sum_{j=1}^{N} g_k(x_j) g_l^*(x_j) = \delta_{kl} N \qquad |k-j| < N \ . \tag{20}$$

Now that the basic properties of Fourier expansion functions have been demonstrated the expansion of a wavefunction $\psi(x)$ is next explored:

$$\psi(x) \approx \sum_{k=-(N/2-1)}^{N/2} a_k e^{i2\pi kx/L} \ . \tag{21}$$

The expansion coefficients a_k become the discrete Fourier expansion coefficients. One can use the orthogonality of the Fourier functions with equidistant sampling points to invert the relation giving

$$a_k = \frac{1}{N} \sum_{j=1}^{N} \psi(x_j) e^{-i2\pi kx_j/L} \ . \tag{22}$$

Thus the adjoint relationship, expressed by the matrix $\mathbf{G}$, is particularly simple. In quantum mechanics the coefficients a_k have an important interpretation since they represent the amplitude of the wavefunction in momentum space. Equation (21) and equation (22) are direct analogues to the continuous Fourier transformation, which changes a coordinate representation to a momentum representation:

$$\psi(x) = \frac{1}{\sqrt{2\pi}} \int_{-\infty}^{\infty} e^{ikx} \bar{\psi}(k) dk \tag{23}$$

$$\bar{\psi}(k) = \frac{1}{\sqrt{2\pi}} \int_{-\infty}^{\infty} e^{-ikx} \psi(x) dx \ . \tag{24}$$

5. Phase Space Representation Of The Fourier Method

At this point the phase space representation of the Fourier method should be considered. The minimum volume in phase space covered by the Fourier representation is calculated as follows: The length of the spatial dimension in phase space is $\mathbf{L}$, and the maximum momentum is $\mathbf{p_{max}}$. Therefore, the represented volume becomes $Volume = 2\mathbf{L} \cdot \mathbf{p_{max}}$, where the factor of two appears because the momentum range is from $-\mathbf{p_{max}}$ to $+\mathbf{p_{max}}$. Using the fact that $\mathbf{p} = \hbar\mathbf{k}$, the phase space volume can be expressed as

$$Volume = 2\hbar\, \mathbf{L} \cdot \mathbf{k_{max}} = Nh \ , \tag{25}$$

where N is the number of sampling points. Since $L = N\Delta x$, it follows that the sampling spacing Δx is related to the maximum wave vector via

$$\Delta x = \frac{\pi}{|\mathbf{k_{max}}|} \ . \tag{26}$$

Figure 1 expresses the relation between the volume in phase space, the unit volume, and the grid parameters Δx and N. The computational scaling properties of the Fourier method are a result of

the scaling properties of the FFT algorithm which scales as $O(N \log N)$. As a result the Fourier method scales with phase space volume as $O(\ Volume\ \log\ Volume\ )$.

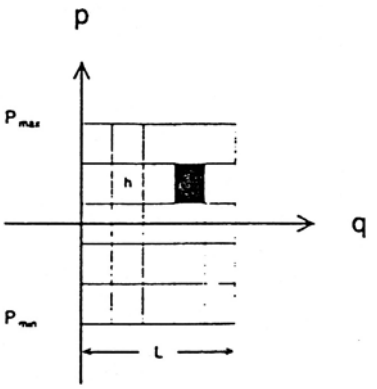

FIG. 1. Phase space volume.

A function that is compact in momentum space is equivalent to the band-limited Fourier transform of the function. Confinement of such a function to a finite volume in phase space is equivalent to a band-limited function with finite support. (The support of a function is the set for which the function is nonzero). The accuracy of a representation of this function is assured by the Whittaker-Kotel'nikov-Shannon sampling theorem [6]. It states that a band-limited function with finite support, is fully specified if the functional values are given by a discrete, sufficiently dense set of equally spaced sampling points. The number of points is determined by equation (25). This implies that a value of the function at an intermediate point can be interpolated with any desired accuracy. This theorem also implies a faithful representation of the n'th derivative of the function inside the interval of support. In other words, a finite set of well-chosen points yields arbitrary accuracy.

For unbounded problems, such as occur in quantum mechanics, the wavefunction cannot be confined in both co-ordinate and momentum space. In principle, no wavefunction is strictly band-limited with finite support. The idea of a wavepacket which is a wavefunction that is almost band-limited is central to the use of the discrete representation. *A wavepacket is a wavefunction that is semilocalized in phase space.* The most well-known example is the Gaussian wavepacket. Although the wavefunction is not confined to a finite volume, the amplitude outside this volume in phase space converges exponentially to zero in either co-ordinate or momentum space. This exponential convergence is typical of a good representation of phase space. A counter-example is supplied by a rectangular packet. In coordinate space the wavefunction is well-confined, but in momentum space the rectangular wavefunction is transformed to $\bar{\psi}(k) = A\frac{\sin(a(k-k_0))}{a(k-k_0)}$, which has only a linear convergence rate with the size of the grid in **k** space. This point is central to the use of the Fourier method which balances the co-ordinate and momentum representations. For a time dependent calculation, a phase space box has to be large enough to keep the wavefunction localized at all times.

6. Representation Of Operators By The Fourier Method

The previous sections have analyzed the dual representation space, *i.e.* a discrete representation in coordinate as well as in momentum space, The the discrete Fourier transform supplies the unitary transformation between the two spaces. The special structure of the two spaces is used to convert the operator mapping of vectors to local operations thus reducing the number of operations from $O(N^2)$ to $O(N \log N)$.

The partition of the Hamiltonian operator into the sum of local operators in coordinate and momentum space is central to the usefulness of the Fourier representation. (Other more complicated examples will be analyzed in section 8). The Hamiltonian operator is usually partitioned into kinetic and potential operators:

$$\hat{\mathbf{H}} = \hat{\mathbf{T}} + \hat{\mathbf{V}} . \tag{27}$$

The numerical strategy is to calculate the operation (mapping) of each of the operators in equation (27) on the wavefunction locally

$$\phi = \hat{\mathbf{H}}\psi = \hat{\mathbf{T}}\psi + \hat{\mathbf{V}}\psi . \tag{28}$$

The potential operator is already local in coordinate space so that its operation is simply $V(x_j)\psi(x_j)$ on grid point j. The Fourier transform allows a local operation of the kinetic energy operator since the expansion functions $g_n(x)$ are eigenfunctions of the kinetic energy operator. The first step in the operation is to Fourier transform $\psi(x)$ from coordinate space to $\bar{\psi}(k)$ in momentum space. The kinetic energy discrete spectrum becomes

$$T(k) = \frac{\hat{\mathbf{P}}^2}{2m} = \frac{\hbar^2 k^2}{2m} . \tag{29}$$

The operation on a component of wavefunction represented in momentum space becomes:

$$\frac{\hat{\mathbf{P}}^2}{2m}\bar{\psi}(k) = \frac{\hbar^2 k^2}{2m} a_k . \tag{30}$$

This result can also be obtained from equation (21) by differentiating the Fourier expansion functions twice by using the discrete version of the relation:

$$\frac{d^n f(x)}{dx^n} = \frac{1}{2\pi}\int_{-\infty}^{\infty} (ik)^n e^{ikx}\bar{f}(k)dk . \tag{31}$$

The result of equations (29)and (30) can be generalized for any local operator in momentum space. The algorithm for calculating the mapping of such operators is as follows: a) calculate the expansion coefficients a_k by the discrete Fourier transform; b) multiply each point in k space by the value of the operator at that point; c) transform the result back to the coordinate sampling space by an inverse Fourier transform. For the Hamiltonian mapping the last step is to combine the operations by summing the action of the potential and kinetic operators.

The convergence of the operator mapping $\phi = \hat{\mathbf{O}}\psi$ is determined by the wavepacket nature of the wavefunction ϕ. The quantum mechanical nature of the approximation depends on the ability to represent the position momentum commutation relation $[\hat{\mathbf{X}}, \hat{\mathbf{P}}] = i\hbar$. A close examination reveals that the function $f(x) = x$ is not band limited on the interval $[0, L]$ because it is discontinuous at the end of the interval $x = L$. Now if $f(x) = x$ is replaced by a periodic function $f(x+L) = f(x)$, then

$$[f(\hat{\mathbf{X}}), \hat{\mathbf{P}}] = i\hbar f'(\hat{\mathbf{X}}) \tag{32}$$

since the Fourier method differentiates exactly periodic functions [13]. This means that the Fourier method fulfills the quantum mechanical commutation relations for periodic potentials and compact wavefunctions. Practically this means that converged results are obtained when the wavefunction is effectively zero at the boundaries of the phase space box *i.e.* it is a wavepacket.

Another important operator which is local in momentum space is the unitary translation operator defined by

$$\hat{\mathbf{U}}_{\mathbf{t}}(y)\psi(x) \;=\; \psi(x+y)\;, \tag{33}$$

which becomes a phase shift in momentum space:

$$\hat{\mathbf{U}}_{\mathbf{t}}(y)\bar{\psi}(k) \;=\; e^{iky}a_k\;. \tag{34}$$

The efficient numerical ability to translate the wavepacket in coordinate space has important consequences. With no loss of accuracy the wavepacket can be centered in the middle of the grid. This can be done continuously, resulting in a dynamical grid, or sequentially at predetermined intervals. Such a process can be accompanied by a shift in momentum

$$\hat{\mathbf{U}}_{\mathbf{p}}(k')\bar{\psi}(k) \;=\; \bar{\psi}(k\;+\;k')\;, \tag{35}$$

which becomes a phase shift in the coordinate space:

$$\hat{\mathbf{U}}_{\mathbf{p}}(k')\psi(x) \;=\; e^{ik'x}\psi(x)\;. \tag{36}$$

The two shift operators equations (33) and (35) can reduce significantly the effective represented volume in phase space by matching the grid to regions where the wavefunction has significant amplitude. One should remember that when shifting the wavefunction the potential has to be shifted in the opposite direction and the kinetic energy operator to $\hat{\mathbf{T}}(k) \;=\; \frac{\hbar^2}{2m}(k-k')^2$. Another use of the shift operator is to interpolate the wavefunction to points which are not represented on the grid. An example of the use of an interpolation procedure is when there is a sudden change of the potential. In photodissociation, for example, the ground state wavefunction is placed on an excited electronic potential which undergoes a rapid momentum increase. To guarantee convergence, the sampling density has to be increased from its value in the ground electronic state.

One simple scheme to effect this interpolation would be as follows. Consider a wavefunction which is sampled by N points. It is first transformed to momentum space. Then the wavefunction is cast onto a larger grid of M points by adding $M-N$ zeros to the momentum values for $|k| \;>\; \pi N/L$. A back transform will increase the density of points without adding any new information to the wavefunction.

The simple implementation of the translation operator is a consequence of a general property of the Fourier transform: a convolution of two functions in coordinate space becomes a multiplication of the transform function in momentum space. This fact can be used to study the mapping of the fourth-order finite difference (FD) kinetic energy operator:

$$\hat{\mathbf{T}}^4_{\mathbf{FD}}\;\psi(x_j) \;=\; -\frac{\hbar^2}{2m}\frac{\psi(x_{j+1})\;+\;\psi(x_{j-1})\;-\;2\psi(x_j)}{\Delta x^2}\;. \tag{37}$$

Equation (37) is a member of the family of convolution operators and therefore is diagonal in **k** space. Performing a Fourier transform, the spectrum in **k** space of the FD kinetic energy operator is obtained:

$$T_{FD}{}^4(k) \;=\; -\frac{\hbar^2}{2m}\frac{2(\cos(k\Delta x)\;-\;1)}{(\Delta x)^2} \;=\; \frac{\hbar^2}{2m}\left(\frac{2\sin(k\Delta x/2)}{\Delta x}\right)^2 \tag{38}$$

Likewise, the sixth-order finite difference operator has the spectrum:

$$T_{FD}{}^{6}(k) = -\frac{\hbar^2}{2m}\frac{2\cos(2k\Delta x) - 32\cos(k\Delta x) + 30}{12(\Delta x)^2} . \quad (39)$$

Figure 2 compares the different spectra.

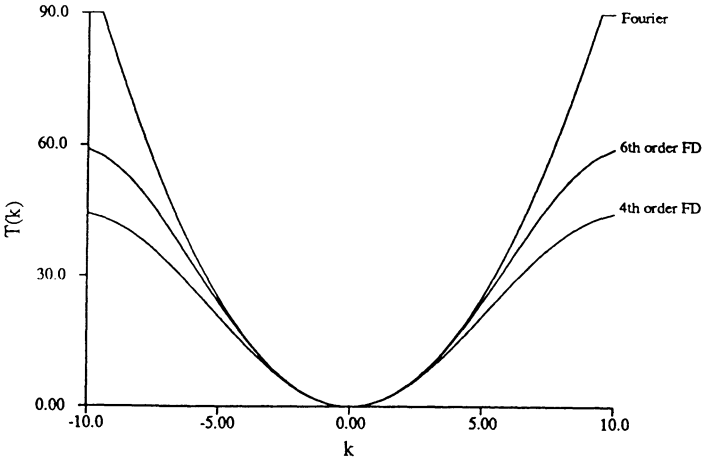

FIG. 2. Comparison of the kinetic energy operator spectrum for the Fourier method and the fourth- and sixth-order finite difference method.

It is apparent that as k increases, the finite difference spectrum deviates more and more from the correct value. It is usually assumed that acceptable accuracy with the FD method is obtained when at least ten points are used per wave period. This means also using ten points per unit volume in phase space. The finite difference algorithms are based on a local polynomial approximation of the wavefunction and therefore the convergence of the method follows a power law of $(\Delta x)^n$ where n is the order of the finite difference approximation. The semilocal description leads to a poor spectral representation of the kinetic energy operator. A general consequence is that a semilocal representation of the momentum operator does not obey the commutation relations of quantum mechanics. This fact, combined with an iterative use of the operator, leads to an exponential accumulation of errors.

7. The Harmonic Oscillator Example

The use of the Fourier expansion method to calculate the spectrum of the Harmonic oscillator demonstrates the properties of the method. For simplicity, consider a harmonic oscillator with mass m and frequency ω. The system is represented by a finite grid with equally spaced sampling points. Figure 3 shows the relevant phase space.

On this grid the maximum value of the potential energy is determined by the extent of the grid,

$$V_{max} = \frac{m\omega^2}{2}\left(\frac{L}{2}\right)^2 = \frac{m\omega^2\Delta x^2 N^2}{8} , \quad (40)$$

where N is the number of sampling points and the grid is centered about zero. The maximum kinetic energy is limited by the maximum momentum which can be represented on the grid leading to

$$T_{max} = \frac{P_{max}^2}{2m} = \frac{\hbar^2}{2m}\left(\frac{2\pi}{2\Delta x}\right)^2 = \frac{\hbar^2\pi^2}{2m\Delta x^2}. \quad (41)$$

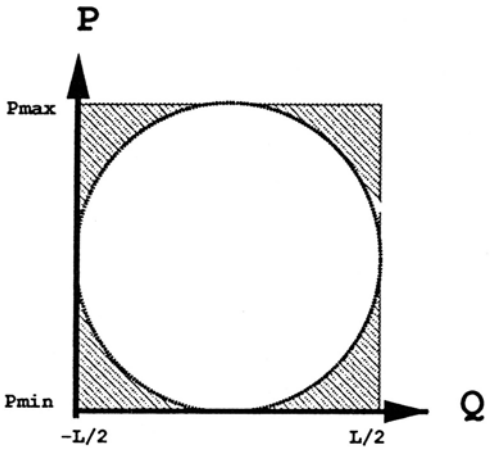

FIG. 3. Schematic phase space of the harmonic oscillator. The ratio between the area of the square and the circle is $\pi/4$.

Equations (40) and (41) represent an energy cutoff due to the discrete representation of the Hilbert space. The optimal representation balances the kinetic and potential energy. Using the virial theorem for the harmonic oscillator, the cutoff in the potential energy should match the cutoff in the kinetic energy, with the resulting optimal grid spacing

$$\Delta x_{opt} = \left(\frac{h}{m\omega N}\right)^{\frac{1}{2}} \quad (42)$$

To illustrate these formulae a grid is constructed using the functions $\psi(x_j) = \delta(x_i - x_j) = \frac{1}{\pi}\mathrm{sinc}(2\pi(x_i - x_j)/\Delta x)$. ($sinc(z) = \sin(z)/z$). This basis function is zero on all other grid points except j where its value is one. The Hamiltonian matrix in this base is calculated as follows: The potential energy matrix is diagonal : $V_{jj} = V(x_j)$. To calculate the kinetic energy matrix elements, a discrete Fourier transform is applied to the expansion function ψ_j then multiplied by $\hbar^2k^2/2m$ and back transformed. The resulting vector becomes the matrix element T_{ji}. At this stage the Hamiltonian matrix $\hat{\mathbf{H}} = \hat{\mathbf{T}} + \hat{\mathbf{V}}$ is diagonalized and the eigenvalues of the discrete representation are compared to the exact results. Table I shows the calculated eigenvalues using 8 , 16 and 32 sampling points with the optimal grid spacing Δx_{opt} for $\omega = 1$, $m = 1$,and $\hbar = 1$.

When the results of the 8 sampling points are compared with 16 sampling points, the exponential convergence of the expansion is demonstrated. For the ground state energy the error decreases six orders of magnitude by only doubling the number of grid points. Other states show similar behavior. When the number of points is doubled again to 32, the error in the ground state becomes saturated because the roundoff error of the double precision arithmetic used in the calculation overcomes the representation error. For unsaturated eigenvalues doubling the number of points from 16 to 32 reduces the error another five to six orders of magnitude.

TABLE I. Convergence of the Fourier representation for the harmonic oscillator

n	Exact	8 points	16 points	32 points
Δx_{opt}		0.8862265	0.6266568	0.4431132
1	0.5	0.4999760107111692	0.4999999998715793	0.4999999999999845
2	1.5	1.500539183698194	1.500000006153576	1.499999999999986
3	2.5	2.494397791604125	2.499999857637178	2.500000000000002
4	3.5	3.534291735531325	3.500002068787167	3.499999999999993
5	4.5	4.378294841394608	4.499978178076544	4.499999999999982
6	5.5	5.960743369677700	5.500169240572392	5.500000000000130
7	6.5	6.212358517586826	6.498928884935602	6.499999999997876
8	7.5	9.976917743504451	7.505122466888302	7.500000000025498
9	8.5		8.478529454896226	8.499999999731434
10	9.5		9.567379412999802	9.500000002414588
11	10.5		10.33263329166096	10.49999998073345
12	11.5		11.95570264326039	11.50000013337068
13	12.5		12.04789296489282	12.49999916184023
14	13.5		14.56012875187433	13.50000457741937
15	14.5		15.44949561677325	14.49997680742042
16	15.5		20.69252130835984	15.50010120025324
17	16.5			16.49957859092886
18	17.5			17.50146417275678

Table II shows the convergence of the first eigenvalues of the finite difference method for the same parameters as table I. The kinetic energy spectrum was constructed from equation (38). The grid spacing Δx was optimized for each case independently.

TABLE II. Convergence of the Finite Difference representation for the harmonic oscillator

Fourth order FD					
n	Exact	8 points	16 points	32 points	64 points
Δx_{opt}		0.7	0.4	0.2	0.11
1	0.5	0.4825740879	0.49478668002	0.49860380104	0.499603845744
2	1.5	1.4317143539	1.47679543400	1.49594408176	1.498464505411
3	2.5	2.2214522909	2.41491682858	2.46274206266	2.490855167811
4	3.5	3.1888159106	3.43350682128	3.54493542145	3.511444750027
5	4.5	3.5308260773	4.10115403608	4.21270019153	4.381333406923
6	5.5	4.4614149311	5.56420368670	5.96798953995	5.712163111633
Sixth order FD					
n	Exact	8 points	16 points	32 points	64 points
Δx_{opt}		0.75	0.44	0.24	0.13
1	0.5	0.496832961	0.4996361441	0.4999643185	0.4999968936
2	1.5	1.485276212	1.4982057984	1.4998077039	1.4999837996
3	2.5	2.393088218	2.485823514	2.4985394570	2.4998518646
4	3.5	3.439160266	3.5084173131	3.5020862644	3.5004457190
5	4.5	3.920284648	4.3402199322	4.4695728153	4.4948505331
6	5.5		5.7031594608	5.5688982555	5.5178475240
7	6.5		6.0977450000	6.2657050814	6.4167645240

Table I and Table II reveal the slow convergence of the finite difference method compared to the Fourier method. Even for the sixth order finite difference the convergence is increased only one order of magnitude when the number of points is doubled. The smaller optimal grid spacing used for the finite difference method should also be noticed.

Another issue is the number of converged eigenvalues that can be obtained in the Fourier method for an n point representation. If the criterion is three significant digits it can be seen from table I that 3 eigenvalues are obtained for 8 points, 8 for 16 points, and 20 for 32 points. It can be concluded therefore that the fraction of significant eigenvalues increases with the number of points in the representation. Figure 4 shows the fraction of significant eigenvalues as a function of the logarithm of the number of points. An eigenvalue is defined as converged when the number of significant digits is larger than a preset value. What can be observed in the figure is that the converged eigenvalue fraction increases with the number of points until it reaches saturation regardless of the number of significant digits used as the convergence criterion. The saturation phenomena occur because the Fourier method constructs a rectangular phase space. Using the balanced choice of Δx_{opt}, the phase space becomes a square. On the other hand, due to energy conservation, the support for an eigenfunction in phase space has the shape of a disc, in the semiclassical limit of large quantum numbers the support area has a shape of a ring, whereas the support for all eigenvalues up to a cutoff energy has the shape of a disc determined by the largest eigenfunction. (or an ellipse in the general case). The area between the circumference of the circle and the perimeter of the square is wasted sampling space. Therefore the maximum sampling efficiency is the ratio of the area of the circle to the area of the square leading to $\pi/4 \approx 79\%$. This is the asymptotic value represented by a bold line in Figure 4.

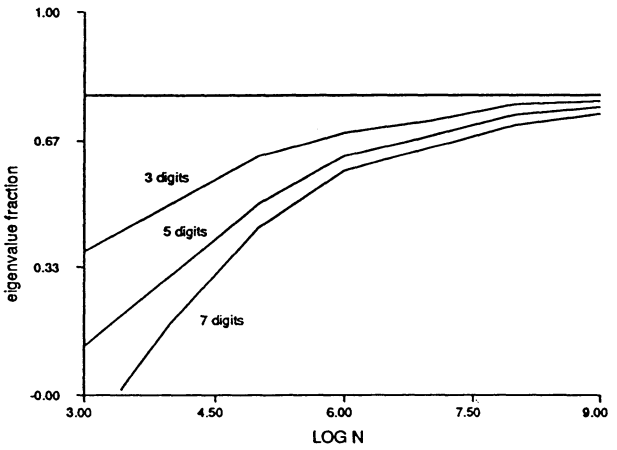

FIG. 4. Sampling efficiency defined by the ratio of converged eigenvlaues within a fixed number of digits to the number of sampling points, as a function of the logarithm of the number of sampling points. The heavy line represents the asymptotic value of $\pi/4$.

To illustrate this point further Figure 5 shows the converged eigenvalue fraction as a function of the grid spacing Δx. It is clear that a square in phase space offers the optimal choice where, to the left of the cusp point $\Delta x = \Delta x_{opt}$ the kinetic energy operator error dominates and to the right of the cusp point the potential error dominates.

This example shows that a careful choice of grid parameters which balance the representation of the kinetic and potential energy can drastically change the amount of computation effort.

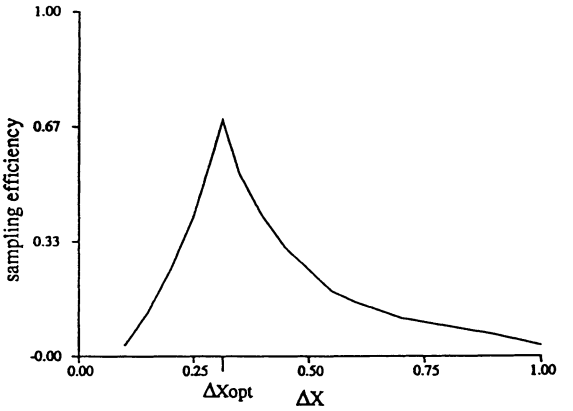

FIG. 5. Sampling efficiency for a fixed number of points ($N = 64$) as a function of the grid spacing Δx.

8. Mapped Fourier Methods

In the previous section the importance of balancing the representation was demonstrated. However even for the optimally balanced representation of the harmonic oscillator there is "air" between the rectangular "box" in phase space used by the Fourier method and the circular shape defined by the Hamiltonian. One can imagine cases where the phase space box has a more complicated shape. For example it can be expected that the optimal sampling density of the Morse oscillator should be lower in regions of small classical kinetic energy. A simple solution to the balancing problem is to define a mapping transformation from the old coordinate system to a new one, x', which can change the sampling density,

$$x' = M(x, \alpha) \tag{43}$$

and its inverse

$$x = M^{-1}(x', \alpha)\,, \tag{44}$$

where α is a set of parameters defining the mapping function M. The result of this mapping is a correlation between the kinetic and potential operators. The computational price of the mapping procedure is that the kinetic energy operator must be calculated by the chain rule

$$\hat{\mathbf{T}} = -\frac{\hbar^2}{2m}\left(\frac{\partial M}{\partial x}\right)\frac{\partial}{\partial x'}\left(\frac{\partial M}{\partial x}\right)\frac{\partial}{\partial x'}\,. \tag{45}$$

This kinetic energy operation can be implemented by a sequential evaluation of the first derivative multiplied by $\frac{\partial M}{\partial x}$. The overall evaulation requires at least 3 Fourier transforms per operation compared to 2 Fourier transforms for the simple, rectilinear, Fourier method. There are many examples of such mapping functions. For example if

$$\theta = \cos^{-1}(x) \tag{46}$$

and

$$x = \cos(\theta) , \tag{47}$$

then the Fourier method is transformed into a Chebyshev pseudo-spectral representation [2]. This representation which belongs to the class of orthogonal polynomial transformations is exceptional because the mapping of equation (47) has a fast transform implementation. Another example is the mapping of the interval $-1 < x < 1$ into itself by the mapping [7]

$$x' = M(x,\alpha) = x'_0 + \frac{1}{\lambda}\tan^{-1}(\alpha_1(x-\alpha_2)) \tag{48}$$

where $x'_0 = (\kappa - 1)/(\kappa + 1)$, $\kappa = \tan^{-1}(\alpha_1(1+\alpha_2))/\tan^{-1}(\alpha_1(1-\alpha_2))$ and $\lambda = \tan^{-1}(\alpha_1(1+\alpha_2))/(1-x'_0)$. The inverse is given by:

$$x = M^{-1}(x',\alpha) = \alpha_2 + \tan((x'-x'_0)/\lambda)/\alpha_1 . \tag{49}$$

The parameters α_1 and α_2 define the center of the region to be stretched and the amount of stretching.

The idea of a functional space which contains a local representation of the kinetic energy operator, can be carried beyond Cartesian coordinates. For example the kinetic energy operator in spherical coordinates is

$$\frac{\hat{\mathbf{P}}^2}{2m} = -\frac{\hbar^2}{2m}\left[\frac{1}{r^2}\frac{\partial}{\partial r}r^2\frac{\partial}{\partial r} + \frac{1}{r^2\sin\theta}\frac{\partial}{\partial\theta}\sin\theta\frac{\partial}{\partial\theta} + \frac{1}{r^2\sin^2\theta}\frac{\partial^2}{\partial\phi^2}\right] . \tag{50}$$

For the ϕ coordinate, the Fourier method is applicable directly. The r and θ coordinates can be evaluated by a sequential application of the Fourier method. An alternative method for the radial part is based on the fact that the Bessel function $J_{1/2}(r)$ is an eigenfunction of the radial part of the Laplacian. This means that by using a Bessel transform the radial part of the Laplacian becomes a local operator with the spectrum $-k^2$. This result can be generalized by using the transform with $J_{l+1/2}$. In this case a centrifugal part $l(l+1)/r^2$, is included in the trasformation. This transform is useful in a mixed calculation when the angular part of the wavefunction is expanded by Y_{lm} functions. Technically, fast Bessel transforms can be carried out by a change of variable. The transform becomes a convolution which is then carried out by means of a fast Fourier transform [16,17]. The Fourier-Bessel transform of order ν is defined by:

$$\hat{\psi}(k) = \int_0^\infty r\psi(r)J_\nu(kr)dr \tag{51}$$

for $k > 0$. The Bessel transform is its own inverse. Substituting $r = r_0e^{-y}$ and $k = k_0e^x$ in equation (51) and multiplying of both sides by $e^{\alpha x}$ gives:

$$e^{\alpha x}\hat{\psi}(k_0e^x) = r_0^2\int_{-\infty}^{\infty} e^{(\alpha-2)y}\psi(r_0e^{-y})e^{\alpha(x-y)}j_\nu(r_0k_0e^{x-y})dy . \tag{52}$$

The expression on the right hand side is a convolution of the function $e^{(\alpha-2)y}\psi(r_0e^{-y})$ and $r_0^2e^{\alpha x}J_\nu(r_0k_0e^x)$. The parameter α is arbitrary and therefore can be chosen to optimize the accuracy. The convolution theorem [18] states that the Fourier transform of the convolution of b and c, $b * c$ equals the product of their Fourier transforms. Hence $b * c$ can be computed by performing an FFT on b and c, multiplying the results, and performing an inverse FFT. The use of the Fourier-Bessel transform can be viewed as a logarithmic mapping function on the coordinates r.

9. The Fourier Method In Many Dimensions

The most straightforward approach in constructing a multi-dimensional representation is to assemble it directly from a product of one-dimensional representations. If, for each dimension, there are N sampling points the computational scaling of the problem of D dimensions becomes $O(DN^D \log N)$ using the Fourier method. The practical meaning of the exponential scaling is that any possible approach which reduces the number of sampling points N and the effective dimensionality should be used.

An obvious solution to minimize N is to introduce symmetry. Consider for example an inversion point such as the point $x = 0$ for the harmonic oscillator. The eigenfunctions can be classified as either being even or odd with respect to parity: $\psi(x) = \pm\psi(-x)$. If one restricts the calculation to one class of functions the computational effort can be reduced by a factor of 2 by using a fast cosine transform for even functions and a fast sine transform for odd functions [8].

Translational symmetry of the type $\hat{\mathbf{V}}(x + nL) = \hat{\mathbf{V}}(x)$ can also be exploited. The symmetry of the potential is reflected in selection rules imposed on the momentum change. A typical example can be found in atom scattering from a crystal surface. In this case the selection rule $\Delta k = \pm n\pi/L$ is imposed. By matching the grid to the unit cell and employing the periodic boundary conditions of the Fourier representation the selection rules are automatically fulfilled. In more than one dimension the matching of the grid to the unit cell might require a skewed grid representation. As will be seen below the skewed grid has more efficient sampling. Other types of symmetry can be considered by working out the selection rules on Δk. Then the kinetic energy operator can be evaluated by shifting the spectrum in k space using equation (36). The details can be found in reference [9].

For more general problems it has been observed that the direct product representation, which for the Fourier method implies a represention by an equally spaced Cartesian grid, is not optimal. A strategy can be developed to enhance the sampling efficiency by abandoning the direct product representation and introducing correlations. A careful analysis of the Fourier method leads to the observation that this direct product grid is not isotropic in momentum space, so that different directions have different sampling intervals. A faithful representation of a multidimensional function by the Fourier method means that the function has to be band limited. The symmetric construction of the coordinate and momentum representation means that the description of the function is also periodic in momentum space. The representation therefore can be viewed as an infinite number of replicas of the original **k** space picture extending in all directions. The band limited property of the original function means that these replicas do not overlap. If *a priori* there is no preferable direction in space a cutoff in momentum can be represented as a sphere with radius p_{max}. A Cartesian grid in coordinate space is also Cartesian in momentum space. Therefore the non overlapping role can be envisioned as packing spheres so that they touch their neighbors at $2D$ points for D dimensions. It is clear that the best sampled direction is in the diagonal one, but for an isotropic problem the volume between the spheres is wasted sampling volume.

Although a completely isotropic grid is not possible, the sampling positions can be chosen to construct the optimum isotropic grid in momentum space. From the previous description it can be concluded that the optimal sampling points are equivalent to the centers of multidimensional densely packed hard spheres. (The problem of the optimal packing of hard spheres has been solved up to 23 dimensions [10]). The free volume between the spheres is wasted sampling volume. The sampling efficiency can be defined as the ratio of the volume of the space filling spheres to the volume of the total space. Figure 6 illustrates the situation in two dimensions.

The Cartesian grid reaches a sampling efficiency of $\frac{\pi}{4} \approx 79\%$. Skewing the grid increases the sampling efficiency to $\frac{\pi}{2\sqrt{3}} \approx 91\%$. In many dimensions, the limit of one sampling point per unit

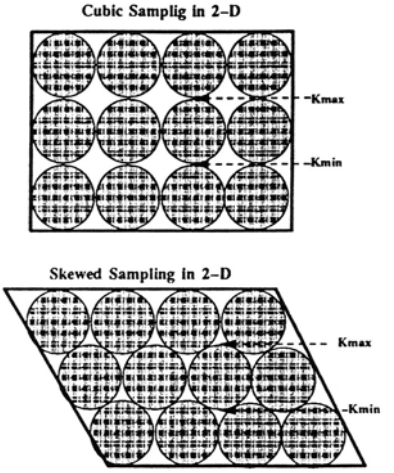

FIG. 6. Schematic view of the k spectrum sampled on a two-dimensional cubic and skewed grid. The fourier transform of a function f is contained in the sphere p_0. Sampling the function the function f on a descrete grid produces copies of $\tilde{f}(K)$ each containing a sphere with radius R. These spheres should be distinct for optimal sampling.

volume is not obtainable even for optimal packing. Table III compares the sampling efficiency of a cubic grid with the optimal grid as a function of dimension.

TABLE III. Isotropic Sampling Efficiency

Dimension	Maximum Efficiency $\eta_{max}(\%)$	cubic lattice η_{cub} (%)	Improvment factor η_{max}/η_{cub}
1	100.0	100.0	1.0
2	90.7	78.5	1.15
3	74.0	52.4	1.4
4	61.7	30.8	2.0
5	46.5	16.45	2.8
6	37.3	8.07	4.6
7	29.57	3.69	8.0
8	8.07	0.505	16.0

Source: Peterson and Middleton [10].

It can be deduced from Figure 7 that the importance of optimal sampling increases with dimensionality. Optimal sampling becomes extremely important for calculations beyond three dimensions. For example for six dimensions, 2.7 sampling points are needed per unit volume, compared to 12.4 points in the Cartesian cubic lattice. Nevertheless even the optimal sampling efficiency decreases with dimensionality. This fact poses an intrinsic limitation to the Fourier method for multidimensional calculations.

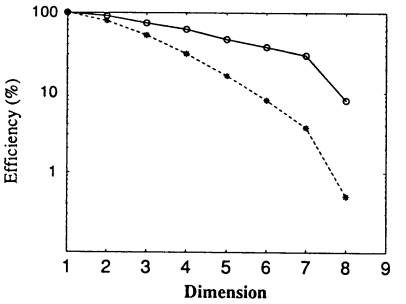

FIG. 7. Comparison of sampling efficiency of a cubic to skewed grid as a function of dimension. The stars represent the cubic grid and the4 open circles the skewed grid.

In a rectangular set of multidimensional coordinates, the kinetic energy operator is separable,

$$\hat{\mathbf{T}} = \frac{\hbar^2}{2m}\sum_{i=1}^{D}\mathbf{K}_i^2 , \tag{53}$$

where $\mathbf{K_i}$ is the vector of k values in the spatial dimension i. In the case of the optimal packing or other skewed sets of coordinates, the kinetic energy operator becomes

$$\frac{\hat{\mathbf{P}}^2}{2m} = \frac{\hbar^2}{2m}\mathbf{K}^{\dagger}\cdot\mathbf{G}\cdot\mathbf{K} , \tag{54}$$

where $\mathbf{K}$ is the vector of k values for each spatial direction and $\mathbf{G}$ a positive definite matrix connecting spatial direction i with direction j. The $\mathbf{G}$ matrix can be calculated by using the knowledge of the coordinates of the centers of the optimally packed spheres [11].

A third option for multi-dimensional calculations is to use non-Cartesian coordinates such as spherical coordinates (equation (50)), cylindrical coordinates, hyperspherical coordinates [9] or bond coordinates [15]. The choice depends on the symmetry of the total Hamiltonian operator as well as the symmetry of the initial condition. These methods are usually implemented by a mixed representation strategy of Fourier decomposition for some degrees of freedom, with some combination of DVR and spectral expansion for the other degrees of freedom.

10. Computational Considerations

The main numerical tool of the Fourier method is the Fast Fourier Transform (FFT). One can view the algorithm as an efficient means to perform the unitary transformation from coordinate to momentum space. An alternative to the FFT algorithm is to define directly the kinetic energy operator in coordinate space

$$\hat{\mathbf{T}}(\mathbf{x}) = \mathbf{Z}^{-1}\hat{\mathbf{T}}(\mathbf{k})\mathbf{Z} , \tag{55}$$

where $\mathbf{Z}_{jk} =< x_j|k >= 1/\sqrt{2\pi}e^{ikx_j}$ is the coordinate to momentum unitary transformation. The drawback to the use of equation (55) is that it is a full matrix operator scaling as $O(N^2)$. Neverthless since the FFT algorithm has an overhead of a factor of 3 to 5 there is a turnover appearing between $N_{crit} = 32$ to $N_{crit} = 96$ so that $N < N_{crit}$ a direct transform becomes more efficient than the FFT algorithm. This finding is very sensitive to the particular computer architecture. For example, very efficient FFT routines are available on vector and parallel computer architecture [14]. One advantage to using the direct matrix kinetic energy operator is that the sampling points in coordinate sapce can be identified thus allowing a correlation with the potential energy operator by eliminating points which are deep in the classically forbidden region. The effect can be achieved also by using the fast Fourier transform programmed with a jagged shaped phase space box.

These findings make it worthwhile to compare the computational strategy used for light and heavy mass quantum calculations. This can be done by considering the effective phase space of the interaction region of reactive scattering. For the H + H_2 reaction with total $J = 0$, the interaction region is approximately contained in a box of dimensions $L = 2 \approx 4bohr$. For energies of $E_{max} \approx 0.1hartree$ a box in momentum space of $p_{max} \approx \sqrt{2mE} = 20a.u.$ contains the action. This means an effective phase space volume of $(80h)^3 \approx 50000h^3$. Such a value is directly related to the number of sampling points or expansion functions required for a converged calculation. The estimate is based on a rectangularly shaped phase space volume. A more complicated shape in phase space which correlates the kinetic and potential energy can reduce the number of sampling points significantly. For this calculation the applicability of the FFT algorithm is marginal.

In multidimensional cases the sampling efficiency of a direct product base is further reduced for two reasons. First, direct product sampling points are not isotropic in kinetic energy. Different directions in space have different sampling efficiencies. Therefore correlated maximally isotropic grids have a much better sampling efficiency where the ratio grows with dimensionality of the problem. Second,correlations in the kinetic and potential couplings improve the sampling efficiency. These considerations lead to a strategy of searching for a tightly tailored grid.

Before examining these options an analogous heavy atom system should be analyzed. As an example of heavy masses, the I_3^- system is typical. A study of its photochemistry shows that due to long range forces the interaction cage is approximately $3 \approx 5bohr$. A typical momentum for a photodissociation energy of 0.1 *hartree* is $p = \sqrt{2mE} = 200a.u.$. This means that a rectangular interaction box in phase space requires about 1000^3h^3 or 10^9 sampling points. This large phase space volume requires a different sampling strategy with particular emphasis on the scaling properties of the sampling method. The difference between the $O(N \log N)$ and the $O(N^2)$ scaling makes the full matrix transform or other methods unusable. The sampling method therefore has to be based on fast transforms.

Two conclusions can be drawn from the analysis. First, for a particular potential sampling, efficiencies close to 1 can be obtained by using a direct matix kinetic energy operator. Second, for a large phase space volume with many sampling points, the difference between sampling strategies becomes smaller so that fast transforms will be a crucial factor.

One of the recurring problems in using the Fourier method is the periodic boundary conditions. In some cases, such as scattering from a crystal surface, these boundary conditions match the physical problem. When a bound state problem is considered, the wavefunction at the boundary should be zero. Effectively such a condition is approximated by forcing the wavefunction at the boundary of the grid to be deep in the classical forbidden region. The amplitude of the wavefunction at the boundary can thus be made exponentially small. Practically this means devoting some sampling points to the classically forbidden region. The extent of this region can be estimated from the semiclassical tunneling formula:

$$\psi(L) \approx e^{-\frac{1}{\hbar}\int_{l'}^{L}\sqrt{2\mu(V(x)-E)}dx} \tag{56}$$

where the buffer region extends from l to L with E as a typical energy. These boundary conditions fit the view of a wavepacket which becomes exponentially close to a band limited function with finite support. Absorbing boundary conditions are also extremely important. Like the bound state

boundary conditions they reduce the amplitude of the wavefunction at the end of the grid to zero. More extensive treatment of this method can be found in chapter [19].

One of the methods to minimize the computational effort is the use of an adaptive grid - a grid which changes as the calculation progresses. For example, in a reactive scattering calculation for the initial state representation it is sufficient to include only the entrance channel; when the wavepacket evolves to sample more of the grid then include the reactive channel. The key element in this program is an interpolation scheme which allows grid-to-grid transfer of the wavefunction. Optimal positioning of the wavefunction is then possible. The collocation method in general and the Fourier method in particular are capable of extremely accurate and efficient interpolation besides their intrinsic advantage in the representation of nonlocal operators. A similar concept makes use of the superposition principle to split the propagation onto two overlapping grids. This method allows the separation of the asymptotic dynamics from the interaction part. Care must be taken that the transmission of amplitude from one grid to the other is gradual in space to avoid numerical problems of overflowing phase space by a sharp transmission function.

11. Summary

The Fourier method has many advantages as well as some drawbacks. Its success in many molecular applications is due mainly to its easy implementation and interpretation. For almost all 1-D and 2-D quantum dynamical calculations one can use an almost generic construction. The Cartesian structure allows a direct interpretation just by inspecting snapshots of the wavefunction either in coordinate space or in momentum space. With its correct use *i.e.* not violating the wavepacket properties of the wavefunction, the Fourier method has extremely high accuracy compared to almost all other methods. Due to the exponential convergence the price paid for this accuracy is not high in computational effort. This accuracy allows the method to be used to calculate isotope effects in tunneling where absolute accuracy of 12 digits is necessary.

In multi-dimensional calculations representation strategy becomes much more involved and computational efficiency becomes a major factor. Except for surface scattering where the Fourier method is the method of choice it seems that a mixed representation strategy on non-Cartesian coordinates might be the optimal method.

Acknowledgments

This work is an accumulation of the efforts of many people, especially Dan Kosloff, Rob Bisseling, and Charly Cerjan. The help of Audrey Dell Hammerich, Meli Nafha, Allon Bartana, and Eyal Fatal is also appreciated. The research was supported by the Binational United States - Israel Science Foundation. The Fritz Haber Research Center is supported by the Minerva Gesellschaft für die Forschung, GmbH München, FRG. Funding from the NATO-ARW is gratefully acknowledged for its support of this conference and these proceedings.

---

[1] J. von Neumann, "Mathematical Foundations of Quantum Mechanics" (Princeton University Press, Princeton NJ 1955)

[2] D. Gottlieb and S. A. Orszag, " Numerical Analysis of Spectral Methods: Theory and Applications" (SIAM, Philadelphia 1977).

[3] J.C. Light I.P. Hamilton J. Chem. Phys. **84** 306 (1986).
[4] J.C. Light I.P. Hamilton and J.V. Lill , J. Chem. Phys. **82**, 1400 (1985).
[5] M. T. Heideman, D. H. Johnson, and C. S. Burrus, IEEE ASSP Magazine 1 no. 4, 14 (1984); C. Lanczos, "Applied analysis" Prentice-Hall, Engelwood Cliffs, NJ (1956); J. W. Cooley, and J. W. Tukey, Math. Comp. **19**, 297 (1965); C. Temperton, C. J. Comp. Phys. **52**, 1 (1983); H. J. Nussbaumer, "Fast Fourier Transform and Convolution Algorithms" 2 nd ed.; Springer Verlag: Berlin, 1982.
[6] E. T. Whittaker, Proc. Roy. Soc. Edinburgh **35**, 181 (1915); H. Nyquist, Trans. AIEE 1 **47**, 617 (1928); C. E. Shannon, Proc. IRE **37**, 10 (1949).
[7] A. Bayliss and E. Turkel, J. Comp. Phys. **101** 349 (1992).
[8] A. Besprozvannaya and D. Tannor Comp. Phys. Commun. **63** ,569 (1991);
[9] Y. Shi and D. Tannor, J. Chem Phys. **92** 2517 (1990).
[10] D. P. Peterson and D. Midelton, Informat. Contr. **5** 279 (1962).
[11] R. H. Bisseling and R. Kosloff, J. Comp. Phys. **76**, 243 (1988).
[12] R. Bisseling and R. Kosloff, J. Comp. Phys. **59**, 136 (1985).
[13] D. Kosloff and R. Kosloff, J. Comp. Phys. **52**, 35 (1983).
[14] P. N. Swarztrauber, in "Parallel Computation" (G. Rodrigue ed.), Academic Press, New York (1982) pp 51.
[15] K. Yamashita and R. Kosloff , in progress (1993).
[16] A. E. Siegman, Optics Lett. **1** 13 (1977).
[17] J. D. Talman, J. Comput. Phys. **29** 35 (1978); Comp. Phys. Commun. **30**, 93 (1983).
[18] R. N. Bracewell, "The Fourier Transform and its Applications" 2nd edition, Mc Graw-Hill, New York (1978).
[19] Please see the chapter in this proceedings by G. G. Balint-Kurti and Á. Vibók.